Available online at www.sciencedirect.com

SciVerse ScienceDirect

Ceramics International 38 (2012) 4385–4389

CERAMICS INTERNATIONAL

www.elsevier.com/locate/ceramint

Short communication

Grain boundary diffusion driven spark plasma sintering of nanocrystalline zirconia

Hanna Borodianska [a,b,c,1], Dmytro Demirskyi [b,2], Yoshio Sakka [a,3], Petre Badica [c,d,4], Oleg Vasylkiv [a,c,*]

[a] National Institute for Materials Science, 1-2-1 Sengen, Tsukuba, Ibaraki 305-0047, Japan
[b] Institute for Problems in Material Science NASU, 3, Krzhizhanovsky Str., 03680 Kyiv-142, Ukraine
[c] Nanyang Technological University, 50 Nanyang Avenue, 639798 Singapore, Singapore
[d] National Institute for Materials Physics, Str. Atomistilor 105bis, Magurele 077125, Romania

Received 8 December 2011; received in revised form 20 December 2011; accepted 21 December 2011
Available online 31 December 2011

Abstract

A methodology is proposed to investigate in detail shrinkage kinetics under isothermal spark plasma sintering (SPS) conditions applied to ceramic nano powders such as Y_2O_3 stabilized ZrO_2. To do so, mild SPS conditions were used (low temperatures and pressure, long dwell times). The extracted experimental activation energy has the value of 246 ± 37 kJ mol^{-1} and the slope of the curves on the intense densification stage is around 0.33. Results are in agreement with densification by a grain-boundary diffusion mechanism as for conventional sintering and the contribution from the specific pressure-assisted mechanisms as for hot pressing is insignificant. This result suggests that exploration of mild SPS might prove rewarding in separation and control of the sintering mechanisms leading to production of specific ceramic with new or improved functionality.

Keywords: Spark plasma sintering; Sintering kinetic; Grain boundary diffusion; Zirconia; Nanopowder; Activation energy

1. Introduction

Spark plasma sintering is attracting significant interest in the recent years for the consolidation of different classes of materials. The method applies simultaneously a uniaxial pressure and a pulsed (and/or dc) current on punches between which in a die (usually from graphite) the powder to be sintered is placed. It is usually accepted that the method is convenient to obtain in the final sintered product a high density close to theoretical values. The method is also usually priced for its ability to realize relatively high heating and cooling rates, this being useful for a better control of the grain particles coarsening during sintering, in many cases minimizing it. Apart from the presented aspects, different authors observed the decrease of the sintering temperature, activated behavior during sintering leading to a reduction of the necessary sintering time, special or significantly improved properties of the SPSed bulks and so on. Several articles and reviews [1–7] show such evidences and take advantage of them. This strongly suggests that *during SPS unconventional non-thermal field-induced effects may occur.* On the other hand, several other articles [8–11] concluded that SPS is rather similar to traditional sintering methods and strongly resembles hot pressing.

Attempts to observe in a more direct manner the processes during SPS were also done, e.g. in works of Aldica et al. [12], and Hulbert et al. [13,14]. Unconventional processes such as formation of plasma states were not observed [13,14], but it is rather impossible to deliver a final general conclusion because of the possible limitations of the experimental techniques, and because of the materials and SPS window-conditions selected for the experiments.

Under presented circumstances it results that search for new approaches on evaluation of the SPS processes is of interest. In

* Corresponding author at: National Institute for Materials Science, 1-2-1 Sengen, Tsukuba, Ibaraki 305-0047, Japan. Tel.: +81 029 859 2673.
E-mail addresses: borodianska@ipms.kiev.ua (H. Borodianska), dxd43@ipms.kiev.ua (D. Demirskyi), sakka.yoshio@nims.go.jp (Y. Sakka), badica2003@yahoo.com (P. Badica), oleg.vasylkiv@nims.go.jp (O. Vasylkiv).
[1] Tel.: +380 44 424 7435; fax: +380 44 424 21 31.
[2] Tel.: +380 44 424 7435; fax: +380 44 424 21 31.
[3] Tel.: +81 029 859 2461.
[4] Tel.: +40 021 3690170; fax: +40 021 3690177.

0272-8842/$36.00
doi:10.1016/j.ceramint.2011.12.064

this work it is proposed to look in detail on the shrinkage kinetics of the intense densification stages of isothermal SPS. To do so, we used a ZrO_2 nanopowder stabilized with Y_2O_3. This is a convenient case study material because there is a significant literature on SPS and traditional sintering of this material and one can compare with our data. Second, we applied low sintering temperatures, long dwell times and a low pressure. These conditions allow expansion of the intense densification and saturation stages of sintering in order to accurately investigate them. They also provide a second dimension of interest. In general, SPS conditions are designed to conduct the processing as fast as possible targeting maximization of the density and minimization of the particle growth. Long time SPS sintering experiments are opposite to the current trend and apparently have no practical sense. For some materials, mild SPS temperature and pressure conditions and long sintering times are suitable not only to avoid coarsening of the particles as in the current work, but might be also important for healing some of the inherent defects resulting due rather harsh and far from equilibrium thermal (e.g. high heating rates) and non-thermal field-induced conditions and processes (e.g. arc discharges if any, formation of hot spots) during the initial SPS stages. Finally, in the estimation of the shrinkage curves calculated from the vertical displacement curves of the punches during SPS we subtracted the displacement curves for empty die system heated in the same conditions as for the case with the powder.

2. Experimental

The zirconia stabilized with 3 mol Y_2O_3 (3YSZ) powder had a primary particle size of 10–50 nm and an aggregates size of 45–70 nm [15,16]. The SPS experiments were performed using 'Dr. Sinter' machine produced by Sumitomo, Japan. A uniaxial pressure of 40 MPa was applied before SPS heating and was kept constant during processing. Heating rate was 80 °C min^{-1} to sintering temperatures of 800, 850, 900, 950, 1000 and 1100 °C. Dwell time was up to 30 min. Vertical displacement of the punches was in situ measured by the SPS machine. After SPS the relative density of the specimens was calculated by dimension to weight estimation, and by the Archimedes method (ASTM B 963-08). Confirmation of approximately constant crystallite and grain size (Fig. 1) during SPS processing was obtained from x-ray diffraction measurements performed at room temperature (Rigaku RINT 2000, Japan, Cu Kα-radiation) using standard Scherer method and by observation of the microstructure by electron microscopy (SEM JEOL JSM 7001F and TEM JEOL JEM-2100-F, Japan).

3. Results and discussion

Relative displacement curves of the punches during SPS for the empty die (D) and for the die filled in were measured. By subtraction of the curves, one obtains the displacement curve for the powder (P) as shown in Fig. 2. The displacement is proportional to shrinkage of the sample in the densification process during SPS and the detail from Fig. 3(a) shows shrinkage on the isothermal SPS heating stage. Clearly there are notable differences between shrinkage as-measured in situ curves by SPS machine and the corrected curve considering behavior of the empty die. Remarkable is that the slope of the corrected shrinkage curve is around 0.33 (Fig. 3(a)). This can be better observed in Fig. 3(b) where the slopes for isothermal SPS at different temperatures are between 0.32 and 0.36, i.e. they are close to 0.33 and can be considered almost constant. Representation from Fig. 2(b) follows the isothermal sintering model [17]:

$$\left(\frac{\Delta L}{L_0}\right)^{n/2} = \frac{F(T)}{2^{n/2}a^{n-m}}t, \tag{1}$$

where a is the radius of the solid particles, $(\Delta L/L_0)$ is the relative shrinkage, $F(T)$ is the function depending on the temperature and materials parameters, n and m are constants typical for each individual mass transport mechanism [17,18], and t is the holding time. The constant n is also the slope of the relative shrinkage curve in log–log representation from Fig. 2(b). For $n = 0.33$ a grain boundary diffusion mechanism is generally considered to be responsible for variation of the relative shrinkage. To confirm this conclusion we extracted the activated energy E using equation:

$$\log\left[\frac{\Delta L/L_0}{T}\right] = \frac{-nE}{RT + C}, \tag{2}$$

where C and n are constants related to the powder geometry and sintering mechanism, respectively and $(\Delta L/L_0)$ is the relative shrinkage at temperature T. Experimental data are presented in Fig. 4 and they follow an approximately linear dependence as expected for Arrhenius-type plots. Activation energy has an average value of 246 ± 37 kJ mol^{-1}. The data presented in

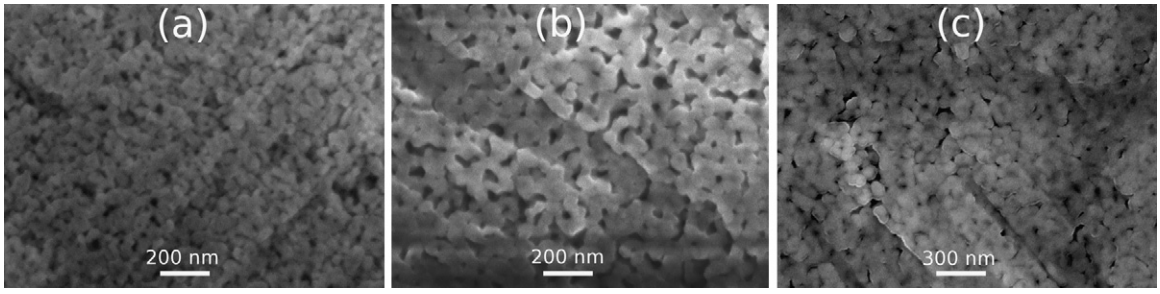

Fig. 1. SEM images of nanoctystalline zirconia after SPS at (a) 800, (b) 900 and (c) 1000 °C for 30 min.

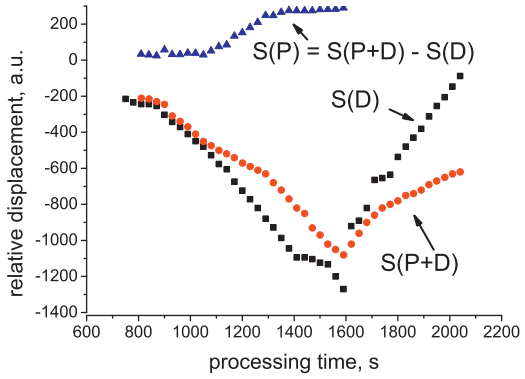

Fig. 2. Vertical punch displacement measured in situ during SPS on empty die (D), and on die filled in with powder (P + D). Displacement for the powder obtained by subtraction of the two experimental curves is also given.

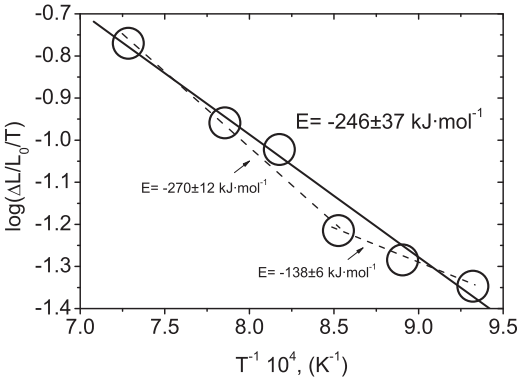

Fig. 4. Arrhenius plot for SPS sintering of nanocrystalline YSZ by the isothermal sintering approach.

Fig. 4 may also indicate on two sintering stages. However, at lower temperatures, activation energy would be −192 kJ mol^{-1}. This value is rather low and there are no similar data reported in the literature. In fact, the average value of 246 kJ mol^{-1} is in the lower values limit when compared to literature (Table 1) [19–25]. Low energy values were reported for conventional sintering of YSZ powders for which grain boundary diffusion mechanism is dominant and, obviously, non-thermal field-induced effects as for SPS are not active. One notes that activation energy depends on the powder. In our case, somehow lower value of E may indicate on some contribution from the field-induced or pressure effects during SPS decreasing E. For SPS processing, Bernard-Granger et al. [8] reported a higher value for E of 450 kJ mol^{-1} than in our case.

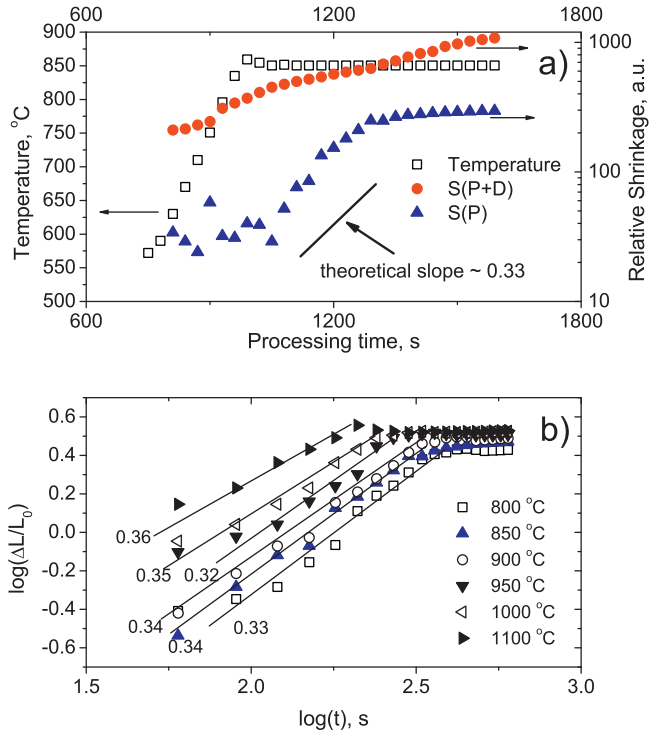

Fig. 3. (a) Shrinkage for the isothermal SPS: as-measured (S(P + D)) and corrected considering behavior of the die (S(P)). (b) Log–log plot of relative shrinkage vs. time at different temperatures.

Estimations were made based on densification kinetics of 3YST granulated powder, but using the nonisothermal conventional sintering approach. Once again, the grain boundary diffusion mechanism is the most probable mechanism during the intense densification stage of SPS.

Despite the agreement between our data of n and E and between our E values and the literature ones, we attempted to simulate for our data a pressure assisted sintering mechanism specific for hot pressing. Within this mechanism relative shrinkage is described by Coble [26]:

$$\left(\frac{\Delta L}{L_0}\right)^n = \frac{F(T)(1 + P_a a/\pi)}{a^m} t, \tag{3}$$

where all parameters are as in Eq. (1) and P_a is the macroscopic applied pressure. In fact, Eq. (1) differs from Eq. (3) with $(1 + P_a{\cdot}a/\pi)$. Therefore Eq. (3) reflects the grain boundary diffusion as well as pressure-induced contribution. Considering the works [26–28], the Arrhenius equation in this case takes the form:

$$\frac{1}{\mu_{eff}} p = K \frac{\exp(-E/RT)}{T} \left(\frac{\sigma_{eff}}{\mu_{eff}}\right)^s, \tag{4}$$

where ρ is $1/L$ (dL/dT), dL/dT is the shrinkage rate, μ_{eff} is the shear modulus of the powder bed, σ_{eff} is the effective stress on the powder bed, K is the a constant described by Bernard-Granger et al. [8], and s is the stress exponent. Expressions for the calculation of μ_{eff} and σ_{eff} are given in Ref. [8] and they

Table 1
Activation energy E values found in literature for conventional sintering and within the grain boundary diffusion mechanism model.

No.	E (kJ mol^{-1})	Material	Ref.
1	615 ± 80	2.8YSZ	[19]
2	377	8YSZ	[20]
3	370	3YSZ	[21]
4	309	$0.16Y_2O_3 - 0.8Zr_{1-x}Hf_xO_2$	[22]
5	300	Nanocrystalline 3YSZ	[23]
6	292	3YSZ	[24]
7	275	Commercial 3YSZ	[25]
8	100	Nanocrystalline 3YSZ	[25]

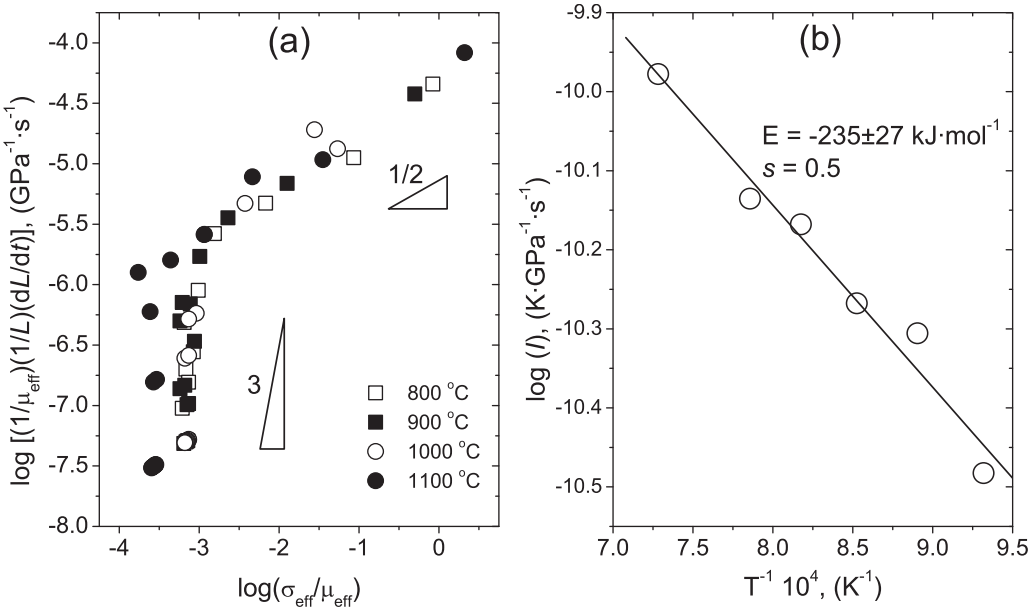

Fig. 5. (a) The densification rate $(1/L)(dL/dt)$ plotted as a function of the normalized effective stress (σ_{eff}/μ_{eff}). (b) Transformed Arrhenius plot for $s = 0.5$.

depend on the Young's modulus of the theoretically dense 3YST taken at 210 GPa [29], the effective Poisson's ratio chosen at 0.31 for the present investigation based on the considerations from Ref. [8], and the macroscopic applied pressure (40 MPa) during SPS. The values of the effective Young's modulus and Poisons's ratio at given densities were calculated according to Lam et al. [30]. To find the value of s, Eq. (4) is transformed for E = constant:

$$\ln\left(\frac{1}{\mu_{eff}}\frac{1}{L}\frac{dL}{dt}\right) = s\ln\left(\frac{\sigma_{eff}}{\mu_{eff}}\right) + K_1, \quad (5)$$

where K_1 is a constant for a fixed sintering temperature. Then the slope of the straight line obtained when drawing Eq. (5) (Fig. 5(a)) corresponds to the s value. Two values for s are obtained of 0.5 and 3. Knowing s-value, from the transformed Eq. (4), i.e. Eq. (6), E can be evaluated:

$$\ln\left[\frac{T}{\mu_{eff}}\left(\frac{\mu_{eff}}{\sigma_{eff}}\right)^s\frac{1}{L}\frac{dL}{dt}\right] = -\frac{E}{RT} + K_2, \quad (6)$$

where K_2 is a constant. The slope of the straight line obtained when representing this equation (Fig. 5(b)) corresponds to the value of $-E/R$.

For $s = 0.5$ or 3, E values are 235 ± 27 kJ mol^{-1} and 760 ± 45 kJ mol^{-1}, respectively. The activation energy value of 760 ± 45 kJ mol^{-1} is rather high for sintering of an YSZ nanopowder when compared with literature data (Table 1). The E values from Table 1 were obtained for conventional sintering without pressure-assistance that normally contributes to the further decrease of the E-values. On the other hand, $E = 760 \pm 45$ kJ mol^{-1} was obtained for $s = 3$ corresponding to the high stress region. But, in our case the applied pressure is rather low (40 MPa). In addition, when high stresses are active, this should induce dislocations in the Nabarro-Herring creep mechanism [18]. Microstructural analysis of our samples did not show the presence of dislocations. A creep mechanism is not active in our case. A similar situation and interpretation was previously given by Satanach et al. for Al_2O_3 [31].

Bernard-Granger et al. [32] reported the densification of granulated zirconia under hot-pressing conditions using a pressure of 100 MPa. As in our present study, the grain growth was assumed to be minimal and there are also two steps with activation energies of 450 ± 25 and 280 ± 25 kJ mol^{-1} for $s = 2$ and $s = 1$, respectively. Although similarities may suggest that a pressure-assisted mechanism of sintering is active during SPS, Jimenez-Melendo et al. [33] concluded that cation diffusion is rate limiting mechanism in the superplastic flow and follows Eq. (7):

$$p = A\frac{\mu \cdot b}{kT}\left(\frac{\sigma}{\mu}\right)^2\left(\frac{b}{d}\right)^2 D_V^{Zr} \quad (7)$$

where $A = 2 \times 10^{-7}$ is a dimensionless constant, b is the Burgers vector, d is the grain diameter and D_v^{Zr} is the volume diffusivity of Zr cations. Considering Eq. (7) the activation energy for creep in zirconia should be between 450 and 700 kJ mol^{-1}. We have seen that for our case the creep is excluded, while for the hot pressing experiments by Bernard-Granger et al. [32] it would be likely more appropriate to consider that the data set $E = 450 \pm 25$ kJ mol^{-1}/$s = 2$ reflects the volume diffusion of zirconia ions that is a pressure dependent mechanism. It results that our data set $E = 760 \pm 45$ kJ mol^{-1}/$s = 3$ does not reflect the real physical situation and, therefore, this data set can be dropped from the analysis. If so, the data set $E = 235 \pm 27$ kJ mol^{-1}/$s = 0.5$ for the low stress region reflects the physical reality. The E value of 235 ± 27 kJ mol^{-1} is close to $E = 246 \pm 37$ kJ mol^{-1} obtained for the grain boundary diffusion model. This result positions SPS, at least for the conditions from this work and

on the intense densification stage, close to a conventional sintering process driven by grain boundary diffusion mechanism, rather than to a fast hot-pressing technique assisted by pressure-induced mechanisms.

4. Conclusions

Isothermal sintering kinetics approach was proposed to be applied for the study of the sintering mechanism during the SPS intense densification stage. It was shown that shrinkage data of the powder sample need correction considering the shrinkage behavior of the die used for SPS processing. The model of grain boundary diffusion mechanism for conventional sintering with the slope of the relative shrinkage curve of 0.33 and activation energy $E = 235 \pm 27\ \mathrm{kJ\ mol^{-1}}$ describes well the intense densification SPS stage. At the same time the contribution from the pressure-assisted specific mechanisms usually active during hot pressing is not significant or does not occur. Mild SPS conditions (low temperatures, long dwell times, low pressures) used to generate the data for the proposed methodology are currently not employed for SPS processing of materials, preference being given to harsh conditions (fast heating, high pressures, short dwell times). This unexplored direction of mild SPS processing deserves further attention since it allows separation and control of different sintering mechanisms, it preserves the initial particle size of the raw powder, and it may generate a specific ceramic with new or improved functionality.

References

[1] D.V. Quach, H. Avila-Paredes, S. Kim, M. Martin, Z.A. Munir, Pressure effects and grain growth kinetics in the consolidation of nanostructured fully stabilized zirconia by pulsed electric current sintering, Acta Mater. 58 (2010) 5022–5030.

[2] J.R. Groza, A. Zavaliangos, Sintering activation by external electrical field, Mater. Sci. Eng. A 287 (2010) 171–177.

[3] S. Grasso, Y. Sakka, G. Maizza, Electric current activated/assisted sintering (ECAS): a review of patents 1906–2008, Sci. Technol. Adv. Mater. 10 (2009) 053001 (24 pp).

[4] Z.A. Munir, D.V. Quach, M. Ohyanagi, Electric current activation of sintering: a review of the pulsed electric current sintering process, J. Am. Ceram. Soc. 94 (2011) 1–19.

[5] R. Raj, M. Cologna, J.S.C. Francis, Influence of externally imposed and internally generated electrical fields on grain growth, diffusional creep, sintering and related phenomena in ceramics, J. Am. Ceram. Soc. 94 (2011) 1941–1965.

[6] P. Badica, A. Crisan, G. Aldica, K. Endo, H. Borodianska, K. Togano, S. Awaji, K. Watanabe, Y. Sakka, O. Vasylkiv, 'Beautiful' unconventional synthesis and processing technologies of superconductors and some other materials, Sci. Technol. Adv. Mater. 12 (2011) 013001.

[7] D. Demirskyi, H. Borodianska, S. Grasso, Y. Sakka, O. Vasylkiv, Microstructure evolution during field-assisted sintering of zirconia spheres, Scripta Mater. 65 (2011) 683–686.

[8] G. Bernard-Granger, C. Guizard, Spark plasma sintering of a commercially available granulated zirconia powder: I. Sintering path and hypotheses about the mechanism(s) controlling densification, Acta Mater. 55 (2007) 3493–3504.

[9] G. Bernard-Granger, C. Guizard, Densification mechanism involved during spark plasma sintering of a codoped α-alumina material: part I. Formal sintering analysis, J. Mater. Res. 24 (2009) 179–186.

[10] J. Langer, M.J. Hoffmann, O. Guillon, Direct comparison between hot pressing and electric field-assisted sintering of submicron alumina, Acta Mater. 57 (2009) 5454–5465.

[11] J.M. Frei, U. Anselmi-Tamburini, Z.A. Munir, Current effects on neck growth in the sintering of copper spheres to copper plates by the pulsed electric current method, J. Appl. Phys. 101 (2007) 114914.

[12] G. Aldica, V. Khodash, P. Badica, J.R. Groza, Electrical conduction in initial field assisted sintering stages, J. Optoelectron. Adv. Mater. 9 (2007) 3863–3870.

[13] D.M. Hulbert, A. Anders, D.V. Dudina, J. Andersson, D. Jiang, C. Unuvar, U. Anselmi-Tamburini, E.J. Lavernia, A.K. Mukherjee, The absence of plasma in 'spark plasma sintering', J. Appl. Phys. 104 (2008) 033305.

[14] D.M. Hulbert, A. Anders, J. Anderson, E.J. Lavernia, A.K. Mukherjee, A discussion on the absence of plasma in spark plasma sintering, Scripta Mater. 60 (2009) 835–838.

[15] O. Vasylkiv, Y. Sakka, Synthesis and colloidal processing of zirconia nanopowder, J. Am. Ceram. Soc. 84 (2001) 2489–2494.

[16] O. Vasylkiv, Y. Sakka, V.V. Skorokhod, Low-temperature processing and mechanical properties of zirconia and zirconia–alumina nanoceramics, J. Am. Ceram. Soc. 86 (2003) 299–304.

[17] R.M. German, Powder Metallurgy Science, 2nd ed., Princeton MPIF, NJ, 1994.

[18] R.M. German, S.J. Park, Mathematical Relations in Particulate Materials Processing: Ceramics, Powder Metals, Cermets, Carbides, Hard Materials, and Minerals, Wiley Interscience, New York, 2008.

[19] J. Wang, R. Raj, Activation energy for the sintering of two-phase alumina/zirconia ceramics, J. Am. Ceram. Soc. 74 (2003) 1959–1963.

[20] W.S. Young, I.B. Cutler, Initial sintering with constant rate of heating, J. Am. Ceram. Soc. 53 (1970) 659–663.

[21] S. Swaroop, M. Kilo, C. Argirusis, G. Borchardt, A.H. Chokshi, Analysis of lattice and grain boundary cation diffusion in 3YTZ using SIMS, Acta Mater. 53 (2005) 4975–4985.

[22] Y. Sakka, Y. Oishi, K. Ando, S. Morita, Cation interdiffusion and phase stability in. polycrystalline tetragonal ceria–zirconia–hafnia solid solution, J. Am. Ceram. Soc. 74 (1991) 2610–2614.

[23] P. Duran, M. Villegas, F. Capel, P. Recio, C. Mour, Low-temperature sintering and microstructural development of nanocrystalline Y-TZP powders, J. Eur. Ceram. Soc. 16 (1996) 945–952.

[24] F. Xue, J. Lu, J. Ma, Theoretical study of densification of nano-sized 3Y-TZP powder: density-grain growth coupling model, J. Nanopart. Res. 11 (2009) 1719–1727.

[25] G.S.A.M. Theunissen, A.J.A. Winnubst, A.J. Burggraaf, Sintering kinetics and microstructure development of nanoscale Y-TZP ceramics, J. Eur. Ceram. Soc. 11 (1993) 315–324.

[26] R.L. Coble, Diffusion models for hot pressing with surface energy and pressure effects as driving forces, J. Appl. Phys. 41 (1970) 4798.

[27] A.K. Mukherjee, J.E. Bird, J.E. Dorn, Experimental correlations for high-temperature creep, Transactions of the ASM 62 (1969) 155–179.

[28] R.K. Bordia, R. Raj, Sintering of TiO_2–Al_2O_3 composites: a model experimental investigation, J. Am. Ceram. Soc. 71 (1988) 302–310.

[29] R.B. Kotelnikov, S.N. Bashlikov, S.G. Galiakbarov, A.I. Kashtanov, High melting-point compounds. A companion, Moscow, Metalurgyia (1969) (in Russian).

[30] D.C.C. Lam, F.F. Lange, A.G. Evans, Mechanical properties of partially dense alumina produced from powder compacts, J. Am. Ceram. Soc. 77 (1994) 2113–2117.

[31] J.G. Santanach, A. Weibel, C. Estournes, Q. Yang, Ch. Laurent, A. Peigney, Spark plasma sintering of alumina: study of parameters, formal sintering analysis and hypotheses on the mechanism(s) involved in densification and grain growth, Acta Mater. 59 (2011) 1400–1408.

[32] G. Bernard-Granger, A. Addad, G. Fantozzi, G. Bonnefont, C. Guizard, D. Vernat, Spark plasma sintering of a commercially available granulated zirconia powder: comparison with hot-pressing, Acta Mater. 58 (2010) 3390–3399.

[33] M. Jimenez-Melendo, A. Dominguez-Rodriguez, A. Bravo-Leon, Superplastic flow of fine-grained yttria-stabilized zirconia polycrystals: constitutive equation and deformation mechanisms, J. Am. Ceram. Soc. 81 (1998) 2761–2776.